Int. J. Solids Structures, 1977, Vol. 13, pp. 925–936. Pergamon Press. Printed in Great Britain

THERMOMECHANICAL RESPONSE OF A VISCOELASTIC ROD DRIVEN BY A SINUSOIDAL DISPLACEMENT

RICHARD W. YOUNG
University of Cincinnati, Cincinnati, OH 45221, U.S.A.

(*Received* 26 *October* 1976)

Abstract—The forced vibrations of a rod of thermoviscoelastic material are studied. The rod is considered to be laterally insulated but not constrained, such that a one-dimensional analysis may be employed. Temperature dependence of the material properties and the resulting thermomechanical coupling effects are included. The vibrations are forced by the imposition of a sinusiodal displacement of known amplitude and frequency at one end of the rod. This problem corresponds to a dissipative material bonded to the surface of a relatively rigid, vibrating structure.

Initial transient behavior is not considered. A steady-state response is found by means of a finite difference formulation. Material properties of a Lockheed solid propellant are used.

The presence of critical frequencies, characterized by high stresses and temperatures, is found for small amplitudes of vibration. Nonlinearities and instabilities lead to a lack of one-to-one correspondence between stress and displacement boundary conditions. No relationship is found between the critical frequencies of the driven rod and the natural frequencies of a rod with an equivalent temperature profile.

INTRODUCTION

Thermomechanical coupling effects can be very important in the oscillatory loading and deformation of viscoelastic materials. During each oscillation mechanical energy is dissipated as heat and the accumulated effect of such dissipation upon the temperature, and consequently upon the material properties, is often significant.

Schapery[1, 2] and Gratch *et al.*[3, 4] have investigated the coupling of the mechanical and thermal equations. Huang and Lee[5] solved the problem of the one-dimensional vibrations of a thermoviscoelastic rod of solid rocket propellant with inclusion of inertia effects. Mukherjee[6] presented a method for obtaining the steady-state response of such a rod which does not require integration in time through the initial thermal transience. He showed that the thermomechanical response was strongly dependent upon frequency of vibration and that excessive heating could occur at certain critical frequencies, even at very low stress levels.

In this paper, the rod problem will be formulated in terms of a boundary condition on displacements, instead of stress, enabling calculation of the displacement as well as stress and strain fields. The response of a layer of material attached to a relatively rigid structure which is vibrating in a known manner would best be analyzed in terms of such a displacement boundary condition. It is found that due to the nonlinearities and subsequent instabilities arising from the thermomechanical coupling, a one-to-one correspondence between stress and displacement boundary conditions does not exist. It will be shown that there are critical combinations of amplitude and frequency of the driving displacement that lead to severe heating and consequent softening of the material. Where applicable, results are compared with those of Mukherjee[7] and are found to be in excellent agreement.

As noted by Huang and Lee[5], replacement of the complex Young's modulus, E^*, by the viscoelastic operator $(\lambda^* + 2\mu^*)$ permits solution of the same problem for an infinite slab.

1. FORMULATION OF THE PROBLEM

Consider a thermoviscoelastic rod of length L which is perfectly insulated along its entire lateral surface, but which experiences no resistance to lateral straining. Distance, x, is measured from the free end of the rod; the end of the rod at $x = L$ is driven by a sinusoidal displacement. At the driven end, the temperature of the rod is assumed to remain at the ambient level, T_0. The Fourier law of heat conduction and Newton's law of cooling are used in prescribing thermal equilibrium at the free end.

The temperature, displacement, strain tensor and stress tensor are written as functions of space and time. The axial stress, $\sigma(x, t)$, is the only non-zero stress component. The strain

tensor consists of the axial strain, $\epsilon(x, t)$, and two equal lateral strains, $\epsilon_L(x, t)$. Only a steady-state analysis will be carried out. It is first assumed that sufficient time has passed to allow the temperature to reach equilibrium; that is, the cycle-averaged temperature is no longer increasing. By such time, all mechanical transients associated with the initiation of the oscillation will have become negligible [4]. It is further assumed, as suggested by Schapery [1], that the cyclic variation of temperature above its mean will also be negligible. Thus the temperature, thermal displacement, and thermal strain may be taken to be independent of time. Complex variable representation is used for quantities which are harmonic in time. It is the real parts of such variables which have physical meaning.

If a displacement of the form $u = u_d e^{i\omega t}$ is imposed at $x = L$, the dependent variables may be written as follows:

$$T(x, t) = T(x) \tag{1}$$

$$u(x, t) = u_T(x) + (u_1(x) + iu_2(x))\, e^{i\omega t} \tag{2}$$

$$\epsilon(x, t) = \epsilon_T(x) + (\epsilon_1(x) + i\epsilon_2(x))\, e^{i\omega t} \tag{3}$$

$$\sigma(x, t) = (\sigma_1(x) + i\sigma_2(x))\, e^{i\omega t} \tag{4}$$

where u_T and ϵ_T are the displacement and strain due to thermal expansion. The strains and displacements are related in the usual manner:

$$\epsilon_T = \frac{du_T}{dx}, \qquad \epsilon_1 = \frac{du_1}{dx}, \qquad \epsilon_2 = \frac{du_2}{dx}. \tag{5}$$

The stresses and strains are related by the complex Young's modulus:

$$\sigma = E^*(T, \omega)\,(\epsilon - \epsilon_T) \tag{6}$$

where

$$E^* = E_1(T, \omega) + iE_2(T, \omega). \tag{7}$$

With the mass density denoted by ρ, the equation of motion becomes:

$$\frac{\partial}{\partial x}(E_1\epsilon_1 - E_2\epsilon_2) = -\rho\omega^2 u_1 \tag{8a}$$

$$\frac{\partial}{\partial x}(E_2\epsilon_1 + E_1\epsilon_2) = -\rho\omega^2 u_2. \tag{8b}$$

The first law of thermodynamics may be expressed in the energy balance equation:

$$(\dot{U} + \dot{E}_K)\, A\,dx\,dt = \frac{d}{dx}\left(\kappa \frac{dT}{dx} A\right) dx\,dt + \frac{\partial}{\partial x}\left[Re(\sigma)\, Re\left(\frac{\partial u}{\partial t}\right) A\right] dx\,dt \tag{9}$$

where U and E_k are the internal and kinetic energies per unit original volume, κ is the thermal conductivity, and A is the cross-sectional area of the rod. Only the real parts of the stress and strain expressions are used in the work term, forestalling a spurious contribution from the product of the imaginary components. Due to the lack of lateral stresses, no work is done by the lateral strains, ϵ_L.

The kinetic energy term may be written as

$$\dot{E}_K = \frac{\partial}{\partial x}[Re(\sigma)]\, Re\left(\frac{\partial u}{\partial t}\right). \tag{10}$$

allowing eqn (9) to be simplified to

$$\dot{U}\,\mathrm{d}t = \kappa\frac{\mathrm{d}^2T}{\mathrm{d}x^2}\,\mathrm{d}t + Re(\sigma)Re\left(\frac{\partial^2 u}{\partial x\partial t}\right)\mathrm{d}t \tag{11}$$

At "steady state," when the system no longer changes from cycle to cycle, integration of $\dot{U}\,\mathrm{d}t$ over one cycle, from $t = t_0$ to $t = t_0 + (2\pi/\omega)$, t_o sufficiently large, yields zero. This, along with substitution from eqns (2) and (4), gives

$$\kappa\frac{\mathrm{d}^2T}{\mathrm{d}x^2} = \frac{\omega}{2}\left(\sigma_1\frac{\mathrm{d}u_2}{\mathrm{d}x} - \sigma_2\frac{\mathrm{d}u_1}{\mathrm{d}x}\right). \tag{12}$$

Using eqns (5)–(7) to eliminate stress and strain from eqns (8) and (12), three equations governing the three functions, u_1, u_2 and T, may be written:

$$\frac{\mathrm{d}}{\mathrm{d}x}\left(E_1\frac{\mathrm{d}u_1}{\mathrm{d}x} - E_2\frac{\mathrm{d}u_2}{\mathrm{d}x}\right) = -\rho\omega^2 u_1 \tag{13a}$$

$$\frac{\mathrm{d}}{\mathrm{d}x}\left(E_2\frac{\mathrm{d}u_1}{\mathrm{d}x} + E_1\frac{\mathrm{d}u_2}{\mathrm{d}x}\right) = -\rho\omega^2 u_2 \tag{13b}$$

$$\kappa\frac{\mathrm{d}^2T}{\mathrm{d}x^2} = -\frac{\omega}{2}E_2\left[\left(\frac{\mathrm{d}u_1}{\mathrm{d}x}\right)^2 + \left(\frac{\mathrm{d}u_2}{\mathrm{d}x}\right)^2\right]. \tag{14}$$

It should be noted that the moduli E_1 and E_2 are functions of temperature and are thus dependent upon x. Given a specific material law, one has three nonlinear, coupled, second-order ordinary differential equations. From the physical statement of the problem, there are six boundary conditions, one on each of the functions at each end of the rod.

2. SOLUTION OF THE PROBLEM

A numerical solution for the problem is found for a Lockheed rocket propellent having the following properties[5, 6]:†

$$E_1 = c_1(c_1^2 + c_2^2)^{-1}\,\omega^{-\beta}(T - T_1)^{-\gamma},\ T > T_1 \tag{15a}$$

$$E_2 = (c_2/c_1)E_1 \tag{15b}$$

where:

$$\begin{pmatrix}c_1\\c_2\end{pmatrix} = \begin{pmatrix}4.61\\1.62\end{pmatrix}\times 10^{-11}\,(\mathrm{psi})^{-1}(\mathrm{sec})^{-\beta}(^\circ\mathrm{F})^{\gamma}$$

$$\beta = -0.214$$
$$\gamma = 3.21$$
$$T_1 = -125^\circ\mathrm{F},$$

and having a density, thermal conductivity, and surface conductance, H, given by:

$$\rho\kappa = 2.12\times 10^{-6}\,(\mathrm{psi})^2\,(\mathrm{sec})\,(^\circ\mathrm{K})^{-1}$$

$$\kappa/H = 3\ \mathrm{in.}$$

The other physical quantities used in this analysis are:

ambient temperature: $T_0 = 65^\circ\mathrm{F}$
rod length: $L = 3$ in.

†In [5], $\kappa = 0.1$ is a misprint, it should read 1.0.

The expressions for the complex modulus are substituted into eqns (13) and (14) and the components of the displacement are written in vector form, $\mathbf{u}(x) = \{u_1(x), u_2(x)\}^T$. At the same time, the equations are put in dimensionless form by defining the following dimensionless spatial coordinate, displacement, temperature and stress:

$$q = x/L \tag{16}$$

$$\mathbf{U} = \mathbf{u}/L \tag{17}$$

$$\tau = (T - T_1)/(T_0 - T_1) \tag{18}$$

$$s_j = \sigma_j/\lambda, \qquad j = 1,2, \text{ where } \lambda = \sqrt{2\kappa\rho(T_0 - T_1)}\sqrt{\omega}. \tag{19}$$

The equations of motion and energy conservation may now be written:

$$\mathbf{U}'' - (\gamma\tau'/\tau)\mathbf{U}' + a_4\tau^\gamma \begin{bmatrix} c_1 c_2 \\ -c_2 c_1 \end{bmatrix} \mathbf{U} = \mathbf{0} \tag{20}$$

$$\tau'' = -(a_5/c_1 a_4)\,\tau^{-\gamma}\,[(U_1')^2 + (U_2')^2] \tag{21}$$

where $'$ denotes d/dq and:

$$a_4 = \rho L^2 \omega^{2+\beta}(T_0 - T_1)^\gamma \tag{22}$$

$$a_5 = c_1 c_2 \rho\omega^3 L^4/[2(c_1^2 + c_2^2)\,\kappa\,(T_0 - T_1)]. \tag{23}$$

Equation (20) is linear in the displacements and, with replacement of $\tau^{-\gamma}$ by an expression involving displacements, eqn (21) will become linear in temperature. The expression for $\tau^{-\gamma}$ takes different forms, depending upon the values of the displacement derivatives. It is first noted that if $U_1' = U_2' = 0$, then τ'' is zero and no expression for $\tau^{-\gamma}$ is needed. Otherwise, manipulation of eqn (20) leads to:

$$\tau^{-\gamma} = a_4\,[c_1(U_1U_2' - U_1'U_2) + c_2(U_1U_1' + U_2U_2')]/U_1'U_2'' - U_1''U_2') \tag{24a}$$

unless $U_1'\,U_2'' = U_1''\,U_2'$, in which case l'Hôspital's rule is applied and:

$$\tau^{-\gamma} = c_2 a_4\,(U_1'U_1' + U_2'U_2')/U_1'U_2''' - U_1'''U_2'). \tag{24b}$$

(Equation (24b) is presented, as will be finite difference approximations for third derivatives, because of repeated need for their use in numerical solution of this problem. In many thousands of calculations, a second application of l'Hôspital's rule was never required.)

With $\tau^{-\gamma}$ replaced, eqn (21) becomes:

$$\tau'' = \frac{a_5[U_1U_2' - U_1'U_2 + (c_2/c_1)\,(U_1U_1' + U_2U_2')]\,(U_1'^2 + U_1'^2)}{(U_1''U_2' - U_1'U_2'')} \tag{25a}$$

or

$$\tau'' = (c_2 a_5/c_1)\,(U_1'U_1' + U_2'U_2')^2/(U_1'''U_2' - U_1'U_2''') \tag{25b}$$

depending upon which form of eqn (24) is needed.

To take advantage of the partial linearity of the equations, an iterative scheme is used. An initial guess for the temperature field is assumed and substituted into eqn (20), which is then solved for U. This displacement field is then used in eqn (25) to calculate the temperature field. The new temperatures are used to recalculate the displacements and the process is repeated until the temperature field converges. Convergence is defined as a change of less than 0.5% at all points.

In practice it was found that direct substitution of the newly calculated temperatures into

the displacement equations led to very slow convergence and often to numerical instability. It became necessary to use a new iterate based on a weighted average of the latest and previous calculations.

Actual solution of eqns (20) and (25) is carried out using finite differences. The rod is divided into N equal intervals by $N+1$ evenly spaced, consecutively numbered mesh points. The $k=1$ and $k=N+1$ points coincide with the free and driven ends of the rod, respectively. The dimensionless mesh point spacing is denoted by δ. The temperature and displacement fields are now represented by arrays of point values, τ_k and U_k.

Substitution of finite difference approximations for the first, second, and third derivatives into eqns (20) and (25) leads to sets of algebraic equations in U_k and in τ_k. Use of finite difference operators of order δ^2 for differentiation leads to very slow convergence and it becomes necessary to formulate the problem in terms of order δ^4 operators.

The finite difference operators used are [8]:

Central differences

$$12\delta F_k' = F_{k-2} - 8F_{k-1} + 8F_{k+1} - F_{k+2} \tag{26a}$$

$$12\delta^2 F_k'' = -F_{k-2} + 16F_{k-1} - 30F_k + 16F_{k+1} - F_{k+2} \tag{26b}$$

$$8\delta^3 F_k''' = F_{k-3} - 8F_{k-2} + 13F_{k-1} - 13F_{k+1} + 8F_{k+2} - F_{k+3}. \tag{26c}$$

Forward and backward differences

$$\mp 12\delta F_{\frac{1}{2}}' = 25F_k - 48F_{k\pm1} + 36F_{k\pm2} - 16F_{k\pm3} + 3F_{k\pm4} \tag{27a}$$

$$12\delta_2 F_k'' = 45F_k - 154F_{k\pm1} + 214F_{k\pm2} - 156F_{k\pm3} + 61F_{k\pm4} - 10F_{k\pm5} \tag{27b}$$

$$\mp 24\delta^3 F_k''' = 151F_k - 720F_{k\pm1} + 1443F_{k\pm2} - 1568F_{k\pm3} + 981F_{k\pm4} - 336F_{k\pm5} + 49F_{k\pm6}. \tag{27c}$$

Special form

If $F'' + G(x, F) = 0$

$$F_{k-1} - 2F_k + F_{k+1} = -\frac{\delta^2}{12}(G_{k-1} + 10G_k + G_{k+1}). \tag{28}$$

The boundary conditions must be reflected in the algebraic systems replacing eqns (20) and (25). They may be expressed as follows:

(1) The temperature of the driven end of the rod remains at the ambient temperature. Thus:

$$\tau_{N+1} = 1. \tag{29}$$

(2) The displacement is prescribed on the driven end of the rod. Thus:

$$\mathbf{U}_{N+1} = \begin{Bmatrix} U_d \\ 0 \end{Bmatrix}, \qquad U_d = u_d/L. \tag{30}$$

(3) The free end of the rod is traction-free. This in turn requires that:

$$\mathbf{U}_1' = \mathbf{0}. \tag{31}$$

(4) The free end of the rod is in radiative thermal equilibrium, thus:

$$H(\tau_1 - 1) = \kappa\tau_1'/L. \tag{32}$$

The finite difference equations arising from eqn (25) are tridiagonal when written in matrix form with the τ_k's as the unknowns. This convenience results from use of the special finite difference operator, eqn (28), and it facilitates solution of the system of equations without use of any numerical matrix inversion techniques.

A similar advantage may be gained in the solution of the equations of motion (eqn 20) by making the following transformation of variables. Let

$$\boldsymbol{\eta} = \tau^{-(\gamma/2)}\,\mathbf{U}, \tag{33}$$

transforming eqn (20) into:

$$\boldsymbol{\eta}'' + \left\{\left(\frac{\gamma}{2}\frac{\tau''}{\tau} - \left(\frac{\gamma}{2}+\frac{\gamma^2}{4}\right)\left(\frac{\tau'}{\tau}\right)^2\right)[I] + a_4\tau^{\gamma}\begin{bmatrix} c_1c_2 \\ -c_2c_1 \end{bmatrix}\right\}\boldsymbol{\eta} = \mathbf{0}. \tag{34}$$

The displacement boundary conditions become:

$$\boldsymbol{\eta}_{N+1} = \begin{Bmatrix} U_d \\ 0 \end{Bmatrix} \tag{35}$$

and

$$\boldsymbol{\eta}_1' + \frac{\gamma}{2}(\tau_1'/\tau_1)\boldsymbol{\eta}_1 = \mathbf{0}. \tag{36}$$

Equation (34) is now in a form such that eqn (28) applies. A set of transfer matrices, $[V_k]$, is defined by:

$$\boldsymbol{\eta}_k = [V_k]\,\boldsymbol{\eta}_{k+1} \text{ for } k = 1,N \tag{37}$$

Application of eqns (28) and (37) to eqn (34) leads to a recursion relation giving $[V_k]$ in terms of $[V_{k-1}]$.†

$$[V_k] = \left\{2[I] - [V_{k-1}] - \frac{\delta^2}{12}(10[B_k] + [B_{k-1}]\,[V_{k-1}])\right\}^{-1}\left\{[I] + \frac{\delta^2}{12}[B_{k+1}]\right\} \text{ for } k = 2,N \tag{38}$$

where:

$$[B_k] = a_4\tau_k^{\gamma}\begin{bmatrix} c_1c_2 \\ -c_2c_1 \end{bmatrix} + \left\{\frac{\gamma}{2}\frac{\tau_k''}{\tau_k} - \left(\frac{\gamma}{2}+\frac{\gamma^2}{4}\right)\left(\frac{\tau_k'}{\tau_k}\right)^2\right\}[I] \tag{39}$$

$$\text{for } k = 1, \quad N+1.$$

$[V_1]$ is found using the transformed third boundary condition. Because eqn (27a) applied to the differentiation of $\boldsymbol{\eta}_1$ in eqn (36) would lead to a very complicated expression for $[V_1]$, in this one case an order δ^2 finite difference operator is used ($2\delta\boldsymbol{\eta}_1' = -3\boldsymbol{\eta}_1 + 4\boldsymbol{\eta}_2 - \boldsymbol{\eta}_3$) and this boundary condition is satisfied only to order δ^2. $[V_1]$ is then given by:

$$[V_1] = \{(\delta^2/12)\,a_6[B_3] - [B_1] + (a_6 - 1)\,[I]\}^{-1}\{2[I] + (\delta^2/6)(2[B_3] + 5[B_2])\} \tag{40}$$

where:

$$a_6 = 3 - \delta\gamma\frac{\tau_1'}{\tau_1}. \tag{41}$$

For a given temperature field, the $[V_k]$ may now be calculated in order, from $k = 1$ to $k = N$. Then the second boundary condition, eqn (35), is applied and the $\boldsymbol{\eta}_k$ are calculated in reverse order, from $k = N$ to $k = 1$. Finally, using eqn (33), the displacements, $\mathbf{U}_k$, are calculated.

†Because the $[B_k]$ are all real-valued matrices of the form $[a\ b/-b\ a]$ the $[V_k]$ will be also and the matrix inversions in eqns (38) and (40) can always be performed.

Solution of the energy equation

With the displacements given, the right-hand side of eqn (25) can be calculated, using eqns (26)–(27). Denoting this quantity as r, one can write $\tau_k'' = r_k$. Then applying eqn (28) and defining

$$p_k = \frac{\delta^2}{12}(r_{k-1} + 10r_k + r_{k+1}), \tag{42}$$

one has:

$$\tau_{k-1} - 2\tau_k + \tau_{k+1} = p_k, \qquad \text{for } k = 2, N. \tag{43}$$

Taking eqn (32) and combining it with eqn (43) for $k = 2,3,4$, and 5:

$$(1+\delta)\tau_1 - \tau_2 = \delta - (13p_2 - 10p_3 + 3p_4)/12. \tag{44}$$

The right-hand side of eqn (44) is taken as a definition for p_1 and manipulation of eqn (43) leads to:

$$\tau_1 = \tfrac{1}{2}\tau_{N+1} - \tfrac{1}{2}\sum_{k=1}^{N}(N+1-k)p_k. \tag{45}$$

τ_{N+1} is given in eqn (29), so the entire temperature field may be calculated from eqns (45), (44), and repeated application of eqn (43).

In this manner, the temperature and displacement fields are calculated interatively until the temperature field converges as previously described. This is initially done for a relatively coarse finite difference mesh with $N = 20$. The mesh is then refined by taking $N = 40$, and the entire process repeated. The final temperature for one mesh size is interpolated and serves as the initial trial for the next mesh size. The refinement is repeated, setting $N = 80$. At that point the convergent temperature field for the latest mesh is compared to that for the previous mesh. If those two fields fail to meet, point by point, the same 0.5% convergence criterion described above, the mesh is again divided and the process repeated. (Convergence was achieved with the 81-point mesh in about half the cases computed. Most other cases converged within a few more mesh divisions, although a few cases near critical frequencies required up to 641 mesh points, the maximum number considered.)

After final temperature convergence is achieved, the displacement field is calculated one last time and the stresses and strains are calculated from these displacements and temperatures.

3. RESULTS AND CONCLUSIONS

Responses to a driving frequency of 10,000 rad/sec were calculated for several different amplitudes of displacement. The results, plotted in the form of maximum temperature vs. position of maximum temperature, are in excellent agreement with results provided by Mukherjee [7] and are presented in Fig. 1. The data provided along the curve give values for the amplitude of the driving displacement and the amplitude of the resulting stress at the driven end. These latter values may be compared with the amplitudes of driving stress used by Mukherjee.

The thermal response of the rod was found to be a highly nonlinear function of the amplitude and frequency of the driving displacement. In Fig. 2, maximum dimensionless temperature, τ_{MAX}, is presented as a function of frequency for an amplitude of $U_d = 0.000153$. At this amplitude, three critical frequencies are present, at $\omega = 2640 \pm 20$ rad/sec, 5990 ± 10 rad/sec, and 8277 ± 3 rad/sec. After the third critical frequency, the maximum temperature climbs rapidly at first and then starts to level off slowly. No data were calculated for frequencies over 30,000 rad/sec due to difficulty in achieving convergence.

Figure 3 shows the end stress as a function of frequency for $U_d = 0.000153$, which varies in much the same manner as the maximum temperature.

Table 1 shows the rapid increases in maximum temperature, stress, and strain as the critical frequencies are passed.

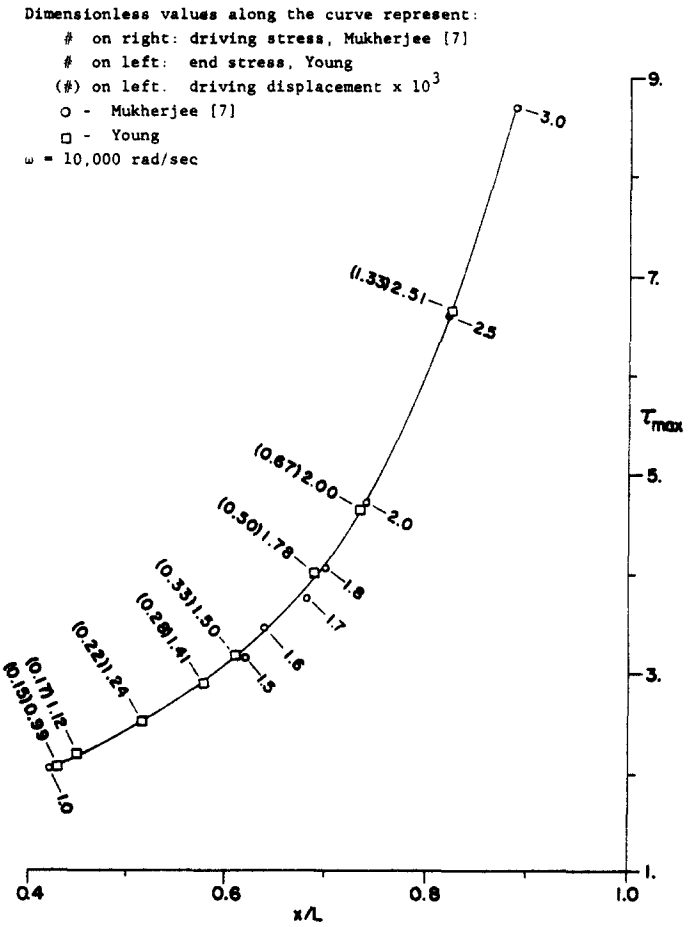

Fig. 1. Maximum temperature vs position of maximum temperature.

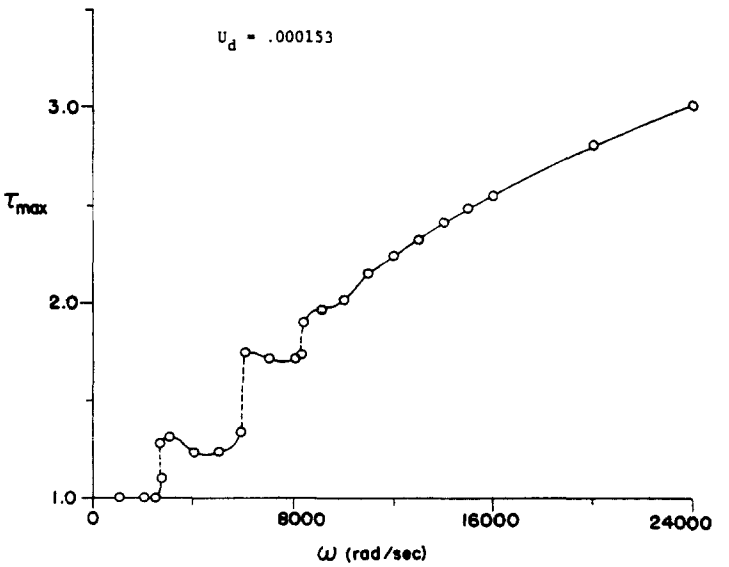

Fig. 2. Maximum temperature vs frequency.

Table 1. Increases in dimensionless response levels at critical frequencies

ω	Temperature	Stress	Strain $\times 10^4$
2640 ± 20	1.118 – 1.294 (16%)	1.53 – 1.77 (16%)	4.72 – 8.69 (84%)
5990 ± 10	1.365 – 1.744 (28%)	0.62 – 1.15 (85%)	6.36 – 13.3 (109%)
8277 ± 3	1.846 – 1.896 (3%)	1.02 – 1.07 (5%)	12.7 – 13.7 (8%)

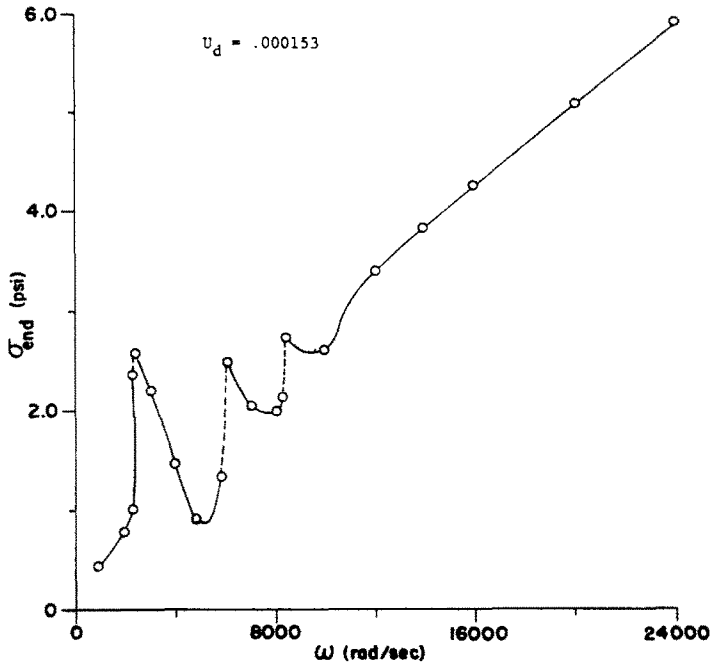

Fig. 3. End stress vs frequency.

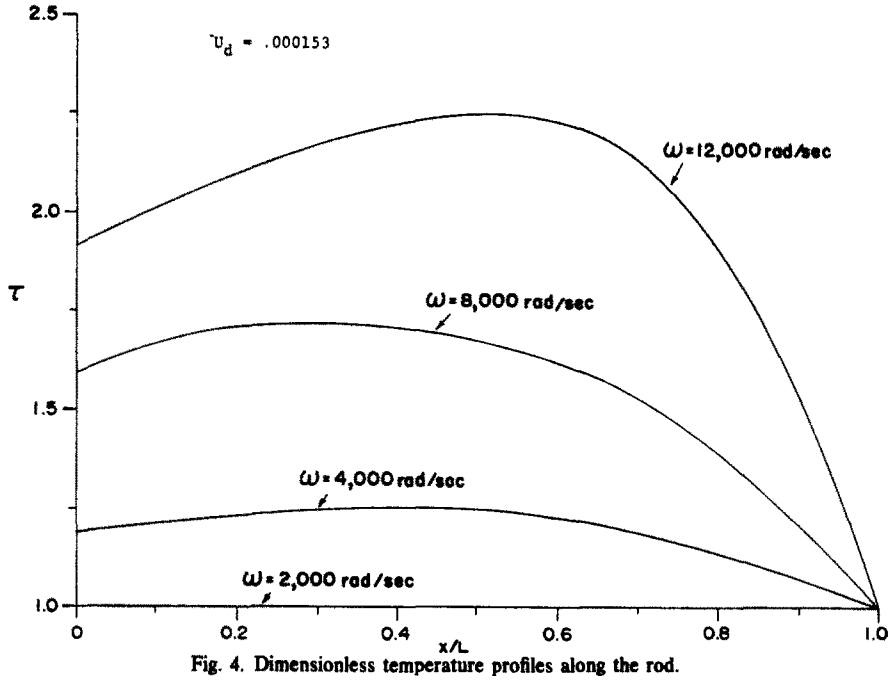

Fig. 4. Dimensionless temperature profiles along the rod.

Figure 4 shows four typical temperature profiles along the rod. The profiles were calculated for an excitation of $U_d = 0.000153$ at four different frequencies. Figure 5 shows the stress profile along the rod, calculated for $U_d = 0.000153$ and $\omega = 12{,}000$ rad/sec. The component labeled "1" is that component in phase with the driving displacement at the driven end.

Figures 6 and 7 show the response as a function of both amplitude and frequency of the

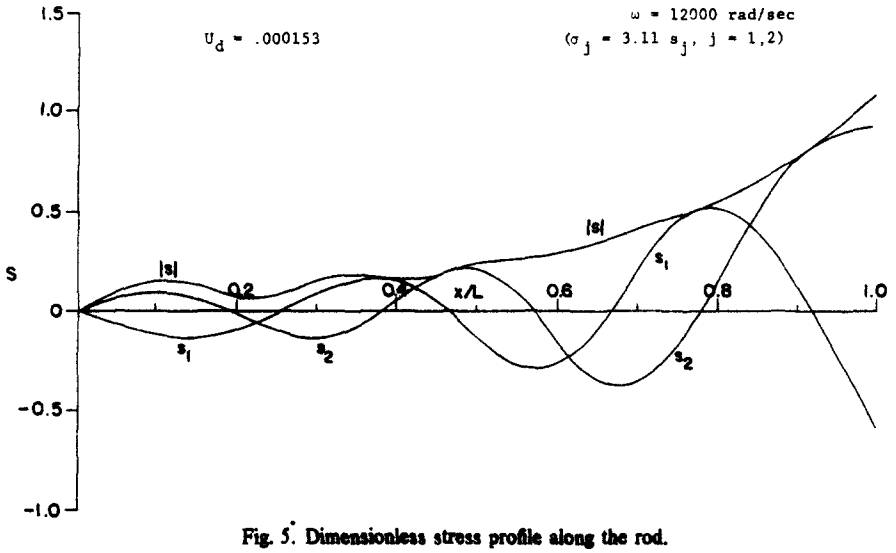

Fig. 5. Dimensionless stress profile along the rod.

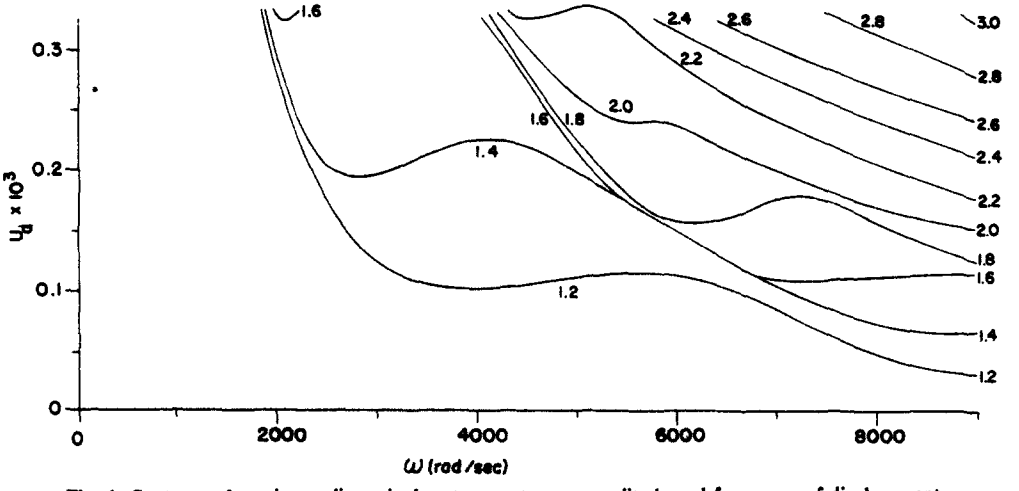

Fig. 6. Contours of maximum dimensionless temperature vs amplitude and frequency of displacement.

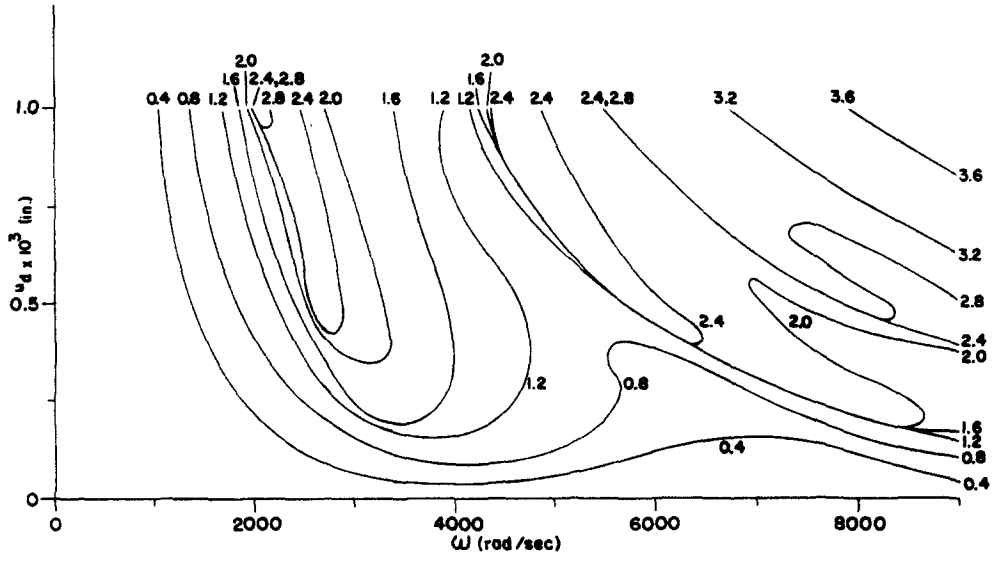

Fig. 7. Contours of end stress (PSI) vs amplitude and frequency of displacement.

driving displacement. In Fig. 6, "contours" of maximum temperature are plotted in the "amplitude-frequency" plane. Although τ_{MAX} increases smoothly with both parameters over much of the range investigated, it is seen that there are certain regions of sharp increase, often followed by a decrease at higher frequencies or amplitudes. It is seen in this figure that the critical frequencies, as discussed earlier, are themselves functions of the driving amplitude, tending to decrease as the amplitude increases. These phenomena are seen even more clearly in Fig. 7, the stress at the driven end of the rod.

As is seen in the figures, the critical frequencies are often characterized by a precipitous jump in the response, indicated by the coincidence of two or more contours. This is a common result in nonlinear vibrations, in which the amplitude of response is no longer a single-valued function of frequency, due to the "folding over" of the resonance peak. Calculations of τ_{MAX} for ω near 6000 rad/sec ($U_d = 0.000153$) show this double-valued response characteristic very clearly. For frequencies between 5940 and 6120 rad/sec, the analysis returns two different temperature and displacement responses, depending upon the initial guess for the temperature profile (see Fig. 8). Multiple solutions such as this, and similar situations in which the response vs. frequency curve is nearly vertical, were the probable causes of the difficulty in achieving good numerical convergence at the critical frequencies.

It can further be seen from Fig. 7 that if one were to drive the rod with a stress of given amplitude, there are regions where three different amplitudes of end displacement are predicted (e.g. $\sigma_{end} = 1.2$ psi, $\omega = 4600$ rad/sec). The two extreme values predicted are both possible solutions, the middle value representing an unstable solution. That the intermediate solution ($u_d = 0.00054$ in.) is unstable can be seen intuitively by noting that if one were to increase the amplitude of the driving stress at a constant frequency, the predicted amplitude of displacement

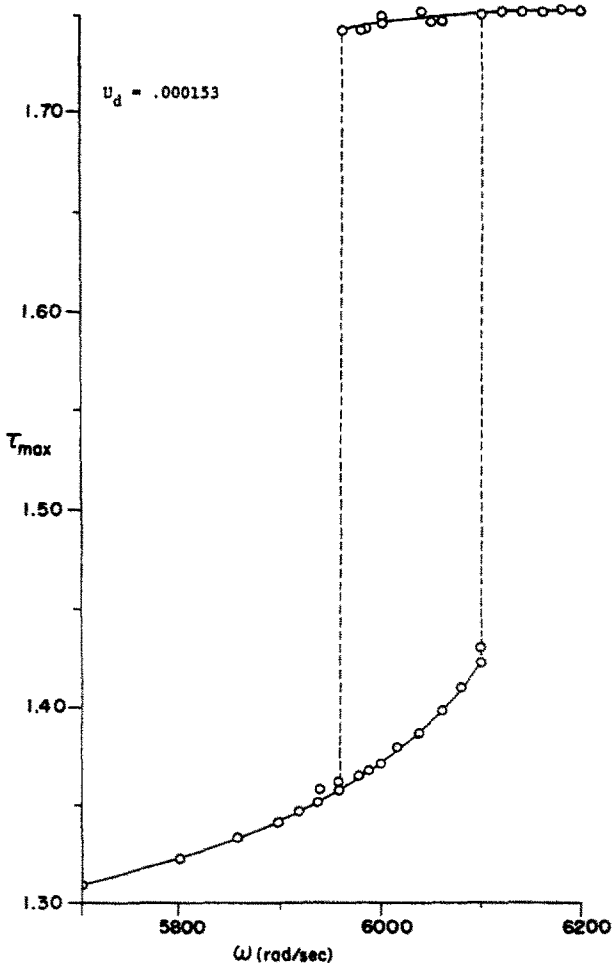

Fig. 8. Discontinuity associated with the second critical frequency.

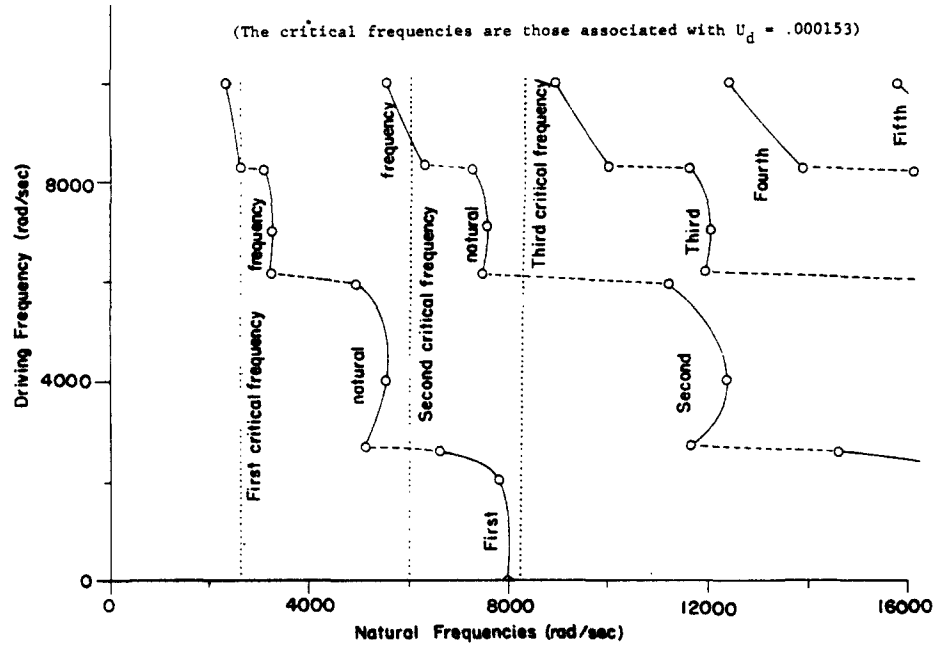

Fig. 9. Natural frequencies of an elastic rod with variable properties.

would decrease. This indicates the fundamental importance of the type of boundary condition imposed on the mathematical problem. If a driving displacement of amplitude 0.00054 in. and frequency 4600 rad/sec is specified, the amplitude of the end stress will be 1.20 psi and the maximum temperature about 125°F. Should however, the rod be driven by the stress at that frequency, a response with an end displacement of 0.0054 in. would not be a stable motion, but instead the end displacement would be either 0.0008 in. or 0.00026 in. (with maximum temperatures of roughly 85° or 200° respectively), depending upon the initial conditions and transient history of the rod. Hence, care should be taken in interpreting results of these figures to determine whether the driving quantity is, in reality, the stress or displacement.

An attempt was made to determine a relationship between the critical frequencies of the rod and the natural frequencies of free vibration of a rod with the same temperature profile, but no such relationship was apparent. For $U_d = 0.000153$, the temperature profiles corresponding to several different frequencies were found, and the natural frequencies of rods with the resulting mechanical properties were calculated. The results of this analysis are shown in Fig. 9. The frequencies along with the vertical axis are those for which the thermomechanical coupling problem was solved. The points plotted are the natural frequencies, as given on the horizontal axis, of the non-uniform rod corresponding to the coupled solution. The dotted vertical lines are the critical frequencies of the coupled problem with $U_d = 0.000153$. Although the lowest natural frequency does tend to associate very weakly with the critical values, the correlation is not very compelling, and the higher frequencies show even less correlation.

REFERENCES

1. R. A. Schapery, Effects of cyclic loading on the temperature in viscoelastic materials with variable properties. *AIAA J.* **2**, 827 (1964).
2. R. A. Schapery, Thermomechanical behavior of viscoelastic media with variable properties subjected to cyclic loading, *J. Appl. Mech.* **32**, (*Trans. ASME* **87** *E*), 611 (1965).
3. R. C. Petrof and S. Gratch, Wave propagation in a viscoelastic material with temperature dependent properties and thermomechanical coupling. *J. Appl. Mech.* **31**, (*Trans. ASME* **86** *E*), 423 (1964).
4. R. M. Wolosewick, S. Gratch, Transient response in a viscoelastic material with temperature dependent properties and thermomechanical coupling. *J. App. Mech.* **32**, (*Trans. ASME* **87**, *E*), p. 620 (1965).
5. N. C. Huang, and E. H. Lee, Thermomechanical coupling behavior of viscoelastic rods subject to cyclic loading. *J. Appl. Mech.* **34**, (*Trans. ASME* **89** *E*), 127 (1967).
6. S. Mukherjee, Thermal response of a viscoelastic rod under cyclic loading. *J. Appl. Mech.* **41**, (*Trans. ASME* **96** *E*), p. 229 (1974).
7. S. Mukherjee, Private Communication.
8. F. B. Hildebrand, *Finite Difference Equations and Simulations*. Prentice Hall, Englewood Cliffs, New Jersey (1968).